# Rate-Equation Analysis of Output Efficiency and Modulation Rate of Photonic-Crystal Light-Emitting Diodes

Shanhui Fan, Pierre R. Villeneuve, and J. D. Joannopoulos

***Abstract*—The performance characteristics of photonic-crystal light-emitting diodes (LEDs) are analyzed, taking into account the effects of both nonradiative recombination and photon reabsorption processes using multimode rate equations. It is shown that, in the presence of strong photon reabsorption, the optimum output efficiency and modulation rates are achieved when the width of the photon density-of-state distribution function is comparable to the width of the spontaneous emission lineshape of the active material. On the other hand, when photon reabsorption is weak, it becomes beneficial to construct high-Q cavities. Based on this analysis, the characteristics of different photonic-crystal LED configurations are discussed.**

***Index Terms*—Dyes, light-emitting diodes, modulation, optical resonators, periodic structures, semiconductor devices, spontaneous emission.**

## I. Introduction

LIGHT emitting diodes (LEDs) are widely used as incoherent light sources in applications such as lighting and short-distance optical fiber communications. An important performance characteristic of an LED is the output efficiency, i.e., the amount of light extracted from the structure at a given input current. In addition, high modulation speed is important for short-distance communications applications, since higher modulation speed implies a larger information capacity.

It has recently been proposed that the output efficiency of LEDs can be significantly improved using a perfectly periodic photonic crystal geometry [1]. There are two principal reasons for this. First, photonic crystals create a band gap in the guided mode spectrum of the LED structure. The guided modes can be completely eliminated within the gap. Second, a photonic crystal creates an upper cutoff frequency for the guided mode spectrum. Thus, in both cases, the emitted light from the active material located inside the crystal can couple only to the radiation modes, resulting in significant enhancement of the light output.

A defect can be introduced into a photonic crystal geometry to form a microcavity [2]. Such a cavity will have a small modal volume and a high quality factor $Q$, which could potentially enhance the rate of spontaneous emission and, therefore, be advantageous for LED applications.[3] The following question naturally arises for photonic-crystal LEDs: Is there an advantage to using a high-$Q$ cavity, or would a high-$Q$ cavity hinder the performance of the LED?

Previous studies of photonic crystal LEDs [1]–[3] have focused on the analysis of the optical modes. The electronic degree of freedom has either not been considered [3], or has been approximated by an idealized dipole moment [1]. More realistic features of the electronic transition have not been incorporated. In particular, to our knowledge, photon reabsorption and nonradiative recombination processes have not appeared in the literature [4].[1]

In this paper, we elucidate the role that photon reabsorption and nonradiative recombination processes play in photonic crystal geometries. We present a rate-equation analysis which incorporates the essential aspects of electronic transitions. We apply the analysis to the output efficiency and modulation rate of photonic-crystal LEDs, taking into account both the photon reabsorption and nonradiative recombination processes. The paper is organized as follows. In Section II, we introduce the basic formalism, which captures the essential features of LEDs. In Section III, we then investigate the effect of photonic crystals on the performance characteristics of LEDs. Finally, the theoretical results are used to discuss a variety of photonic-crystal LED structures in Section IV.

## II. Formalism

We shall study LED structures using rate equations. We consider a system made up of a group of upper electronic levels, and a group of lower electronic levels. The equations describe the dynamics of the total population $n$ of carriers in the upper levels, and the number of photons in the $i$th optical mode $p_i$, as follows:

$$\frac{dn}{dt} = E - \sum_i (A_i n - d_i p_i) - \Gamma n \tag{1}$$

$$\frac{dp_i}{dt} = A_i n - d_i p_i - \gamma_i p_i. \tag{2}$$

Here, $A_i$ is the spontaneous emission rate into the $i$th optical mode, $\Gamma$ is the nonradiative decay rate of the population of carriers in the upper levels, and $d_i$ and $\gamma_i$ are the absorption and output coupling rate of photons in the $i$th optical mode, respectively.

Equations (1) and (2) are closely related to similar equations used in describing microcavity LEDs and lasers [5]–[7]. In con-

Manuscript received September 22, 1999; revised June 29, 2000. This work was supported by the MRSEC Program of the National Science Foundation under Grant DMR-9400334.

The authors are with the Department of Physics, Massachusetts Institute of Technology, Cambridge, MA 02139 USA.

Publisher Item Identifier S 0018-9197(00)08141-0.

[1]After the manuscript was submitted, we became aware of the reference.

trast to previous work, we treat here all optical modes within the spontaneous lineshape explicitly and on an equal footing, rather than focusing on the behavior of a single lasing mode while averaging the effects of all other modes.

For a two-level atomic system where the transition is homogeneously broadened, it can be shown from the Einstein relation that [8]

$$d_i = A_i n_0 \tag{3}$$

where $n_0$ is the occupation number of the lower level. In such a case, the spontaneous emission coefficient and absorption coefficient possess identical lineshapes. For realistic material systems, such as semiconductor or organic emitters, both the lower and the upper levels can be inhomogenously broadened. Population distributions in the lower and upper levels have to be taken into account explicitly in order to determine the correct relation between absorption and spontaneous emission spectra [9]. Equation (3) no longer holds. In this paper, we do not assume a two-level system, but rather incorporate explicitly both the spontaneous emission spectra and the absorption spectra of the active material.

We relate parameters $A_i$ and $d_i$ to properties of bulk materials. First, we note that, in a bulk material,

$$A_i = \frac{A \cdot F_0(\omega_i)\, d\omega}{V \cdot \rho_0(\omega_i)\, d\omega} \tag{4}$$

where

$A$ $\equiv \sum_i A_i$; total spontaneous emission rate;
$V$ normalization volume;
$F_0(\omega_i)$ normalized lineshape function;
$\rho_0(\omega_i)$ density of photon states for the uniform bulk.

Also, from (2), in the absence of external pumping and output coupling, the number of photons in state $i$ can be shown to decay as

$$p_i(t) = p_i(0) e^{-d_i t}. \tag{5}$$

Hence, the absorption coefficient $\alpha(\omega_i)$ is related to the absorption rate $d_i$ as:

$$\alpha(\omega_i) = \frac{r d_i}{c} \tag{6}$$

where $r$ is the index of refraction, and $c$ is the speed of light in vacuum.

In LED structures, the dominant effect on the total spontaneous emission rate is a change in the density of states, while the spontaneous emission rate into any individual state remains largely unaltered [10]. We can, therefore, use (4) to estimate the rate constant $A_i$ using measured bulk properties. This procedure will allow us to relate the LED performance to actual material parameters.

## III. Analysis

To study the output efficiency and modulation rate of an LED structure, we need to calculate the photon output rate $S_i$ from the $i$th optical mode, which is defined as

$$S_i = \gamma_i p_i \tag{7}$$

and measures the number of photons that escape the high-index light-emitting structure per unit time. In studying the extraction efficiency, we use a time-independent excitation $E$, and study the number of photons coming out of the structure. For the study of modulation, we assume that the excitation has a harmonic temporal dependence, i.e., $E \sim Ee^{j\omega t}$. By investigating the analytic properties of $S_i$ as a function of frequency, we can obtain the temporal response properties.

### A. Output Efficiency

Using (1) and (2), and a time-independent excitation $E$, the output rate from the $i$th optical mode is determined to be

$$S_i = \frac{A_i \cdot \dfrac{\gamma_i}{\gamma_i + d_i}}{\displaystyle\sum_i \left( A_i \cdot \frac{\gamma_i}{\gamma_i + d_i} \right) + \Gamma} \cdot E. \tag{8}$$

We note that the spontaneous emission rate $A_i$ is accompanied by a factor $(\gamma_i/\gamma_i + d_i)$, which implies that the presence of photon reabsorption, effectively speaking, reduces the spontaneous emission rate. Also, realistic LED devices always involve multimode output. Appropriate summation over the "relevant modes" is, therefore, required in order to correctly study the output behavior. Since what constitutes the "relevant modes" is dependent upon the application, below we study output characteristics in different application scenarios.

*1) Display and Lightning Applications:* For applications such as display or lighting, it is usually desired to get as much light out of the structure as possible over the entire spontaneous emission bandwidth. In a photonic crystal LED, a bandgap is opened in the guided mode spectrum [1]. Within the gap, all the optical modes are radiation modes. Thus, when the spontaneous emission frequencies fall inside the gap, all available optical modes contribute to the output. We, therefore, sum over all available states to obtain the output, as given by

$$S = E \cdot \frac{\displaystyle\sum_i \left( A_i \cdot \frac{\gamma_i}{\gamma_i + d_i} \right)}{\displaystyle\sum_i \left( A_i \cdot \frac{\gamma_i}{\gamma_i + d_i} \right) + \Gamma}. \tag{9}$$

In the absence of nonradiative recombination, i.e. $\Gamma = 0$, the extraction efficiency would be unity. Even the photons that are reabsorbed by the atomic system would eventually be reemitted and contribute to the output signal. When the nonradiative recombination is present, on the other hand, reabsorbed photons may eventually be lost through nonradiative processes. In order to achieve high output efficiency, it is clear from (9) that the *effective* total spontaneous emission rate

$$A_{\text{eff}} \equiv \sum_i \left( A_i \cdot \frac{\gamma_i}{\gamma_i + d_i} \right) \tag{10}$$

has to dominate the nonradiative recombination rate $\Gamma$.

The relative rate of the radiative and nonradiative processes can be modified using a high-$Q$ cavity. Here, $Q$ is related to $\gamma$ by $Q = \omega_c/(2\gamma)$, where $\omega_c$ is the center frequency. Methods for creating high-$Q$ cavities are presented in Section IV. We

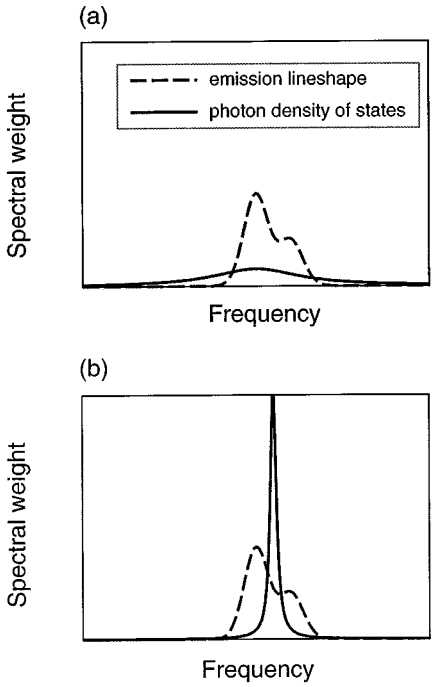


Fig. 1. Two cases comparing the material emission lineshape with the photon density of state lineshape. (a) The material lineshape is much narrower than the photon density of state lineshape. (b) The material lineshape is much wider than the photon density of state lineshape.

begin by studying a simple situation where the photon reabsorption process can be ignored. Such a situation could occur for organic emitters, for example, where the energy levels of the molecules could be designed such that the absorption and spontaneous emission are spectrally separated [11]. We consider the effect of a resonant cavity in two limiting situations, as shown in the two panels of Fig. 1. In Fig. 1(a), the spontaneous emission linewidth is much narrower than the cavity linewidth. $A$ can thus be approximated by

$$A \approx \rho(\omega_{\text{transition}}) \int d\omega A(\omega) \tag{11}$$

where $\omega_{\text{transition}}$ is the center frequency of the emission linewidth. Raising the cavity $Q$ increases the density of states $\rho(\omega_{\text{transition}})$ at the resonant frequency of the cavity, and indeed enhances the total spontaneous emission rate.

In the opposing limit, as shown in Fig. 1(b), the spontaneous emission linewidth is much larger than the cavity linewidth. The total rate $A$ is instead approximated by

$$A \approx A(\omega_c) \int d\omega \rho(\omega) = A(\omega_c) \tag{12}$$

and is in fact pinned to the rate at the resonant frequency of the cavity. Narrowing the cavity linewidth beyond the material emission linewidth does not further enhance the total spontaneous emission rate.

For most semiconductor systems, both the absorption and emission processes occur between the conduction and valence bands. Significant absorption exists at the emission wavelengths. Photon reabsorption processes, therefore, cannot be ignored in general. From (10), photon reabsorption results in the reduction of the effective spontaneous emission rate for the $i$th mode by a *reabsorption factor* $(\gamma_i/\gamma_i + d_i)$. This factor decreases monotonically as the cavity $Q$ is increased. In the low-$Q$ limit, where $\gamma \ll d_i$, the reabsorption factor approaches unity and photon reabsorption processes play no significant role. Photon reabsorption processes become important when the output coupling rate $\gamma_i$ is comparable to the reabsorption rate $d_i$. In the high-$Q$ limit, reabsorption dominates over output coupling, and the effective spontaneous emission rate and, hence, the output efficiency, approach zero.

By inserting (4) and (6) into (10), we find

$$A_{\text{eff}} = \int \left( \frac{AF(\omega)}{\rho_0(\omega)} \cdot \rho(\omega) \cdot \frac{\gamma}{\gamma + \dfrac{c\alpha(\omega)}{r}} \right) d\omega. \tag{13}$$

Here,

$$\rho_0(\omega) = \frac{\omega^2}{\pi^2 (c/r)^3} \tag{14}$$

is the density of states in the bulk material. In the photonic crystal, since the photonic bandgap suppresses guided modes at the emission frequencies, the only available optical modes within the gap are free-space vacuum modes and cavity modes. The density of states $\rho(\omega)$ for the crystal is, therefore, assumed to consist of two parts

$$\rho(\omega) = \frac{\omega^2}{\pi^2 c^3} + \frac{1}{\pi V_m} \cdot \frac{\gamma}{(\omega - \omega_c)^2 + \gamma^2}. \tag{15}$$

The first part in (15) is the free-space vacuum modes, while the second part describes a cavity mode with center frequency $\omega_c$, width $\gamma$, and modal volume $V_m$.

We now present numerical examples for two important classes of light-emitting material systems, semiconductors and organic dyes. More specifically, we investigate GaAs and DCMII [11] material systems. Examples of the use of DCMII in light-emitting devices can be found in [11] and [12]. These two material systems are chosen since their emission properties are distinctively different. In GaAs, strong absorption occurs at the emission frequencies while, for DCMII, the absorption and emission peaks are spectrally separated.

The spontaneous and absorption spectra of GaAs at room temperature are taken from [13], and plotted in Fig. 2. The spontaneous emission spectrum peaks at a frequency 1.42 eV, with a full-width-at-half-maximum of 0.05 eV. The ratio between the center frequency and the width defines $Q_{\text{material}}$. In the case of GaAs, we find $Q_{\text{material}} \sim 28$. The refractive index is taken to be 3.4. We assume a resonance mode with frequency centered at the peak of the spontaneous emission spectra, and a modal volume of $2 \cdot (\lambda_{\text{peak}}/(2r))^3$, where $\lambda_{\text{peak}}$ is the center wavelength. Such a small modal volume is experimentally achievable in a photonic crystal system [14].

The resulting $A_{\text{eff}}$ as a function of $Q$ is calculated using (13), and plotted in Fig. 3. At the low-$Q$ limit, which corresponds to a cavityless structure, the effective spontaneous emission rate is reduced from that of the bulk value by a factor $(1/r)^3$, i.e., $A_{\text{eff}} = (1/r)^3 A = 0.025$ A for the specific case where $r = 3.4$. The presence of the photonic bandgap results in a significant reduction of the density of photon states. Consequently, the spon-

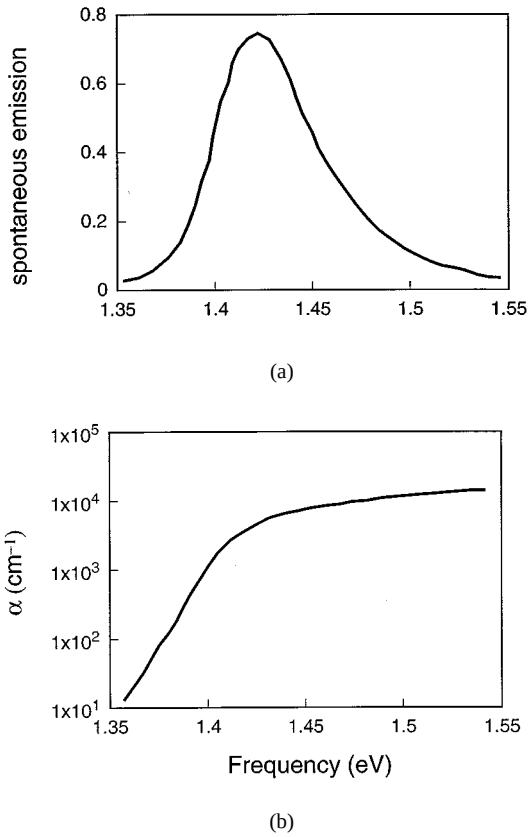


Fig. 2. Material properties of GaAs, as taken from [13]. (a) Spontaneous emission spectra. (b) Absorption coefficient.

taneous emission rate is greatly reduced from the uniform bulk value. The density of photon states increases with $Q$. For small values of $Q$, photon reabsorption is not significant, and $A_{\text{eff}}$ rises with $Q$. A maximum of 0.92 A is reached at a $Q$ of 30, which is very close to $Q_{\text{material}}$. When $Q$ becomes significantly larger than $Q_{\text{material}}$, photon reabsorption becomes important, and the effective spontaneous emission rate decreases with further increase of $Q$.

We vary the nonradiative recombination rate $\Gamma$ from 0.1 to 0.3 A and calculate the corresponding output efficiency, as plotted in Fig. 4. The choice of $\Gamma$ here corresponds to an internal quantum efficiency varying from 90% to 78%, which is achievable in semiconductor systems [15]. The output efficiency shows the same qualitative behavior as $A_{\text{eff}}$. Maximum output is achieved when the $Q$ of the structure is comparable to $Q_{\text{material}}$, and increasing $Q$ beyond $Q_{\text{material}}$ reduces the output efficiency. These quantitative results are consistent with the qualitative behavior discussed earlier.

The spontaneous emission spectrum of DCMII is taken from [11], and plotted in Fig. 5. The absorption is negligible throughout the emission wavelengths. The emission peak is centered at a frequency of 2 eV with a width of 0.25 eV. Assuming that these dyes are embedded in a high-index environment with a refractive index of 3.4, and that the resonance mode is centered at the frequency of the emission peak with a modal volume of $2\cdot(\lambda_{\text{peak}}/(2r))^3$, we calculate $A_{\text{eff}}$ according to (13) and plot the values in Fig. 6.

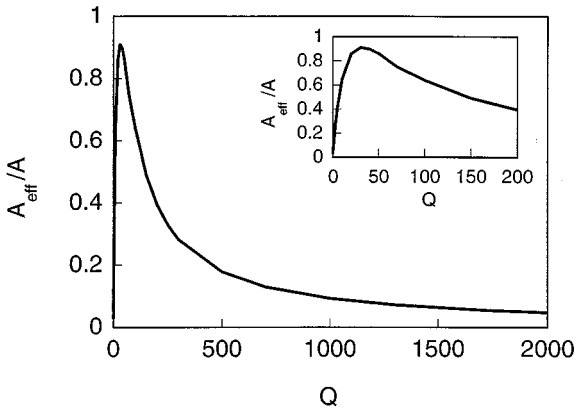


Fig. 3. Effective spontaneous emission rate as a function of $Q$, for a photonic crystal LED structure using GaAs as the active material.

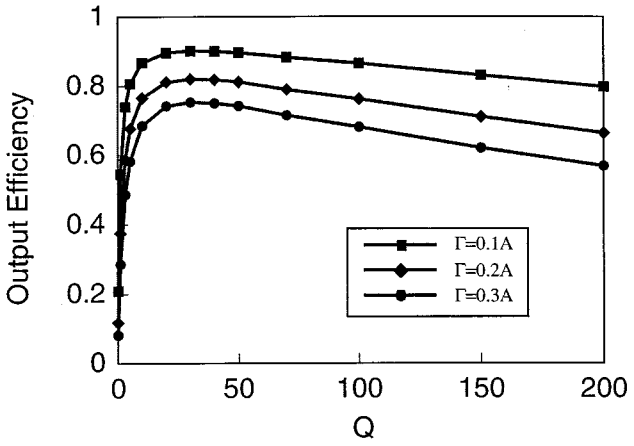


Fig. 4. Total output efficiency as a function of quality factor, for a photonic crystal LED structure using GaAs as the active material.

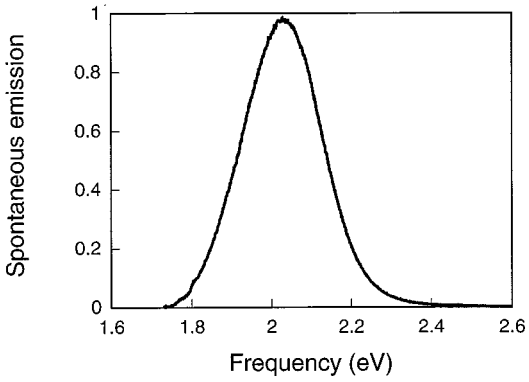


Fig. 5. Spontaneous emission spectrum of DCMII, as taken from [11].

In the low-$Q$ limit, the spontaneous emission rate is reduced from the bulk value by a factor $(1/r)^3$, similar to the semiconductor case. However, in contrast with the semiconductor case, $A_{\text{eff}}$ increases monotonically with $Q$, and saturates when $Q \gg Q_{\text{material}}$ at a value of 1.3 A. The output efficiency, calculated with $\Gamma$ ranging from 0.1 to 0.3 A, is plotted in Fig. 7. The results exhibit the same saturation behavior as $A_{\text{eff}}$. Hence,

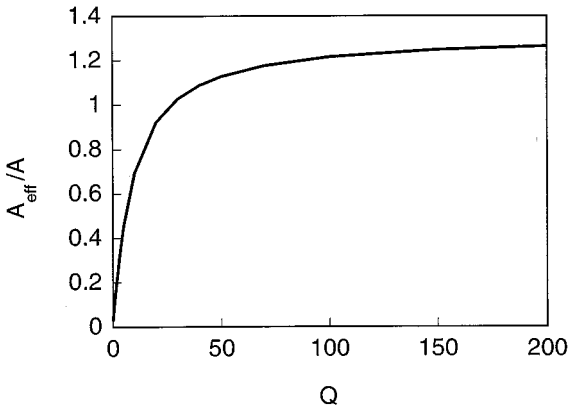


Fig. 6. Effective spontaneous emission rate as a function of $Q$, for a photonic crystal LED structure using DCMII as the active material.

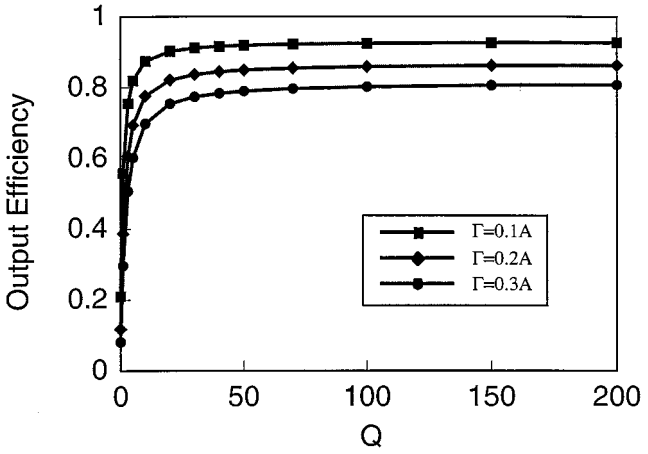


Fig. 7. Total output efficiency as a function of $Q$, for a photonic crystal LED structure using DCMII as the active material.

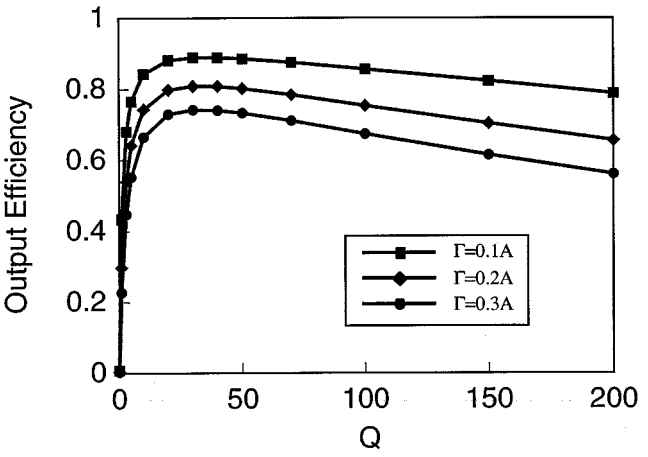


Fig. 8. Output efficiency from the cavity as a function of $Q$, for a photonic crystal LED structure using GaAs as the active material.

when photon reabsorption is absent, it becomes beneficial to construct high-$Q$ cavities in order to enhance the output efficiency and the spontaneous emission rate. Such enhancement, however, saturates when $Q \gg Q_{\text{material}}$.

Often photonic crystal point defects are constructed with the purpose of increasing the effective total spontaneous emission rate. Depending upon the property of the material system, however, the enhancement might not always be achievable, as can be seen by comparing Figs. 3 and 6. In general, enhancement can be best achieved in systems where photon reabsorption is weak, and where the spontaneous emission lineshape is narrow.

*2) Communications Applications:* Communications applications may require the use of a high-$Q$ resonant cavity to narrow the emission linewidth below the natural emission linewidth of the material, in order to further improve the temporal coherence property of the emitted light. For this purpose, the cavity linewidth is necessarily smaller than the material linewidth, characteristic of the regime shown in Fig. 1(b). Here, however, we are primarily interested in the output from optical modes that are controlled by the cavity. The output rate $S$ is computed by summing the numerator only over the cavity modes

$$S = E \cdot \frac{\sum_{\text{cavity}} \left( A_i \cdot \frac{\gamma_i}{\gamma_i + d_i} \right)}{\sum_i \left( A_i \cdot \frac{\gamma_i}{\gamma_i + d_i} \right) + \Gamma}. \tag{16}$$

Since the cavity linewidth is narrow, we assume that the spontaneous emission rate $A_i$ and the photon decay rates $\gamma_i$ and $d_i$ do not vary appreciably over the cavity lineshape. Equation (16) can then be simplified as

$$\begin{aligned} S &\approx E \cdot \frac{A(\omega_c) \cdot \frac{\gamma}{d+\gamma}}{\sum_i \left( A_i \cdot \frac{\gamma_i}{\gamma_i + d_i} \right) + \Gamma} \cdot \int \rho(\omega)\, d\omega \\ &= E \cdot \frac{A(\omega_c) \cdot \frac{\gamma}{d+\gamma}}{\sum_i \left( A_i \cdot \frac{\gamma_i}{\gamma_i + d_i} \right) + \Gamma} \end{aligned} \tag{17}$$

where we assume that the cavity supports a single resonance such that $\int \rho(\omega)\, d\omega = 1$. Interestingly, the behavior of a single-mode cavity resembles that of a single photon state as described in (8).

Using (16), we calculate the efficiency of extracting light from the cavity, using the material parameters of GaAs and DCMII. The results are presented in Figs. 8 and 9, respectively. Except in the limit of $Q \to 0$, the density of cavity states is always much larger than that of the vacuum states, as can be seen from (15). The output from the structure is, therefore, dominated by the cavity output. The qualitative features of Figs. 8 and 9 thus closely resemble the total output from the structure, as shown previously in Figs. 4 and 7. In the case where photon reabsorption is important (Fig. 8), the output reaches a maximum when $Q \sim Q_{\text{material}}$. On the other hand, in the absence of photon recycling (Fig. 9), the output from the cavity increases monotonically as a function of $Q$, and saturates in the high-$Q$ limit.

For certain applications in communications, one might instead be primarily interested in enhancing the spectral density

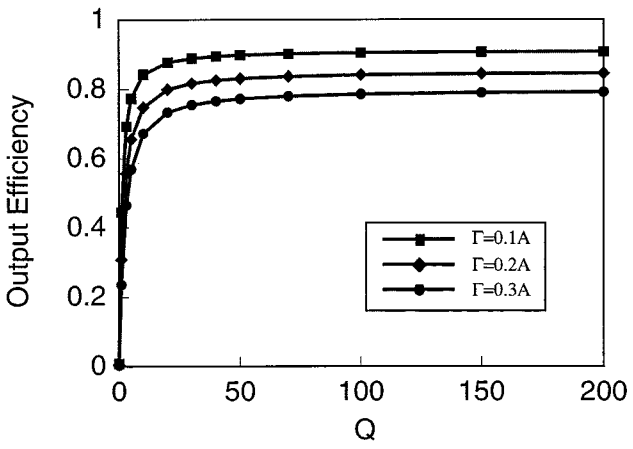


Fig. 9. Output efficiency from the cavity as a function of $Q$, for a photonic crystal LED structure using DCMII as the active material.

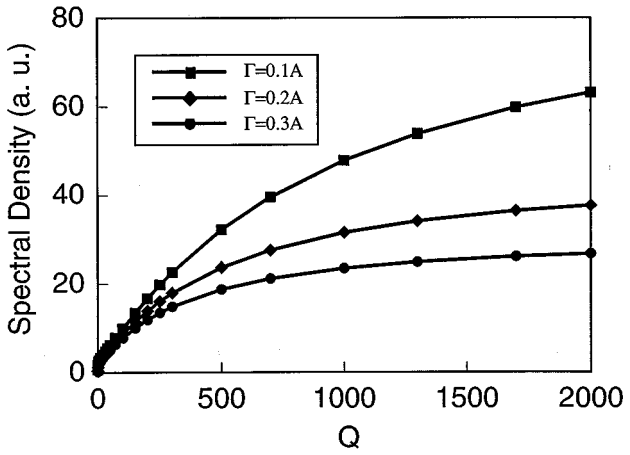


Fig. 10. Spectral density $P(\omega_0)$ as a function of $Q$, for a photonic crystal LED structure using GaAs as the active material.

of the output light $P(\omega_0)$ at a given frequency $\omega_0$. Following the derivations that lead to (17), we have

$$P(\omega_0) = E \cdot \frac{\sum_i \left( A_i \cdot \frac{\gamma_i}{\gamma_i + d_i} \delta(\omega_i - \omega_0) \right)}{\sum_i \left( A_i \cdot \frac{\gamma_i}{\gamma_i + d_i} \right) + \Gamma} = E \frac{A_\omega \cdot \frac{\gamma}{d+\gamma}}{\sum_i \left( A_i \cdot \frac{\gamma_i}{\gamma_i + d_i} \right) + \Gamma} \rho(\omega_0). \quad (18)$$

$P(\omega_0)$ can be increased by introducing a cavity with a resonant frequency centered at $\omega_0$, such that $\rho(\omega_0) = (1/\pi\gamma)$. In this case, the spectral density becomes

$$P(\omega_0) = E \frac{A_{\omega_0} \cdot \frac{1}{d+\gamma} \pi}{\sum_i \left( A_i \cdot \frac{\gamma_i}{\gamma_i + d_i} \right) + \Gamma}. \quad (19)$$

Using (18), we calculate $P(\omega_0)$ for the cases of GaAs and DCMII. The results are shown in Figs. 10 and 11, respectively. In both cases, the spectral density increases monotonically with $Q$. In the case where strong photon reabsorption is present (Fig. 10), the spectral density saturates with increasing $Q$, since both the numerator and the denominator approach a constant in the high-$Q$ limit. We note that the saturation threshold can be much higher than $Q_{\text{material}}$. Here, the level-off occurs when both conditions $\gamma < d$ and $\sum_i (A_i \cdot (\gamma_i/\gamma_i + d_i)) < \Gamma$ are satisfied. When nonradiative recombination processes are weak, the latter condition determines the saturation threshold.

In the absence of photon reabsorption (Fig. 11), the spectral density increases linearly with $Q$ in the high-$Q$ limit. Here, the numerator in (19) increases linearly, while $A_{\text{eff}} = \sum_i (A_i \cdot (\gamma_i/\gamma_i + d_i))$, and hence the denominator, approaches a constant (Fig. 7). Using a high-$Q$ cavity is, therefore, effective in enhancing the spectral density.

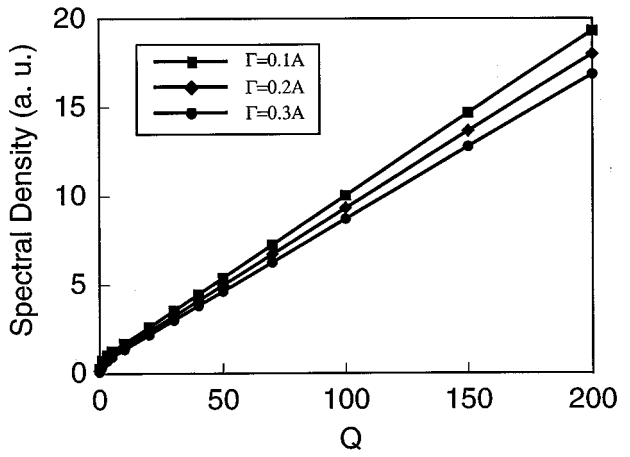


Fig. 11. Spectral density $P(\omega_0)$ as a function of $Q$, for a photonic crystal LED structure using DCMII as the active material.

### B. Modulation Rate

For communications applications, an important characteristic of an LED is the modulation speed. We first focus on the response behavior of a single optical mode. As we show later, all the optical modes in the LED structures have approximately the same modulation characteristics. Assuming a harmonic modulation of the pumping rate $E = Ee^{j\omega t}$, the output in the $i$th optical mode can be written as

$$S_i(\omega) = \frac{A_i \gamma_i}{j\omega + \gamma_i + d_i} \cdot \frac{1}{j\omega + \sum_i \left( A_i \frac{j\omega + \gamma_i}{j\omega + \gamma_i + d_i} \right) + \Gamma} \cdot E. \quad (20)$$

When photon reabsorption processes are negligible, i.e., $d_i = 0$, and (20) has two poles in the complex $\omega$ plane. Both poles are located on the imaginary axis, one at $\omega = -j(\gamma_i + d_i)$, and the other at $\omega = -j(\sum_i A_i + \Gamma)$. The first one characterizes the rate at which the photon number in the $i$th optical mode decreases in the LED structure, while the second pole characterizes the rate of electronic recombination. The response time of the combined

electron–photon system is determined by the slower of the two processes.

The period of the light at a wavelength (in vacuum) of 1.55 $\mu$m is roughly 5 fs. Photonic crystals offer the possibility of designing cavities with a wide range of $Q$s [14], [16], [17]. In the case where $Q \sim 1000$, the photon lifetime is on the order of several picoseconds. For modes that are not associated with a high-$Q$ resonance, the photon lifetime typically is on the order of a few femtoseconds. Electronic recombination times, on the other hand, are typically on the order of nanoseconds in semiconductor [13] and organic dyes [18]. Since the modulation speed is limited by the slower of the two processes, the electronic recombination rate, which is a sum of the total spontaneous emission rate and the nonradiative recombination rate, clearly constitutes the limiting factor.

It is important to point out that the modulation property of a single optical mode is determined by the *total* spontaneous emission rate, rather than the spontaneous emission rate into the mode under consideration. Therefore, different optical modes, despite the difference in photon decay time, will have approximately the same modulation characteristics, as dictated by the slower electron recombination process. Summation over relevant modes, as we have done when discussing different output scenarios, will not affect the response characteristics.

To increase the modulation speed, it is, therefore, important to increase the total spontaneous emission rate. In the case where photon recycling is absent, such as the case of DCMII, the behavior of $A_{\text{eff}}$ has been discussed in detail in the previous section (Fig. 6). The maximum modulation rate is enhanced when the $Q$ of the structure is increased. Such an enhancement saturates when the quality factor of the structure significantly exceeds $Q_{\text{material}}$.

In the presence of photon reabsorption, the poles of the function $S_i(\omega)$ can be obtained by solving the following equation:

$$j\omega = \sum_i \left( A_i \frac{j\omega + \gamma_i}{j\omega + \gamma_i + d_i} \right) + \Gamma. \tag{21}$$

Again, the modulation rate is determined by the pole with the smallest imaginary part, the position of which can be approximated by

$$j\omega_{pole} \approx \sum_i \left( A_i \frac{\gamma_i}{\gamma_i + d_i} \right) + \Gamma. \tag{22}$$

Equation (22) is a self-consistent solution of (21), since $\omega_{pole}$ as determined by (22) is far smaller than the photon decay rates $\gamma_i$ and $d_i$. The modulation rate is, therefore, determined by the total effective spontaneous emission rate $A_{\text{eff}}$, the behavior of which, in the presence of strong reabsorption, has been discussed in detail in the previous section, using GaAs as an example (Fig. 3). Optimum modulation rate is achieved when the material linewidth and the cavity linewidth become comparable.

As can be seen by comparing Figs. 3 and 6, depending upon the property of the material system, a photonic crystal may either enhance or suppress the maximum modulation rate. In general, enhancement can be best achieved in systems where the photon reabsorption effect is weak, and where the spontaneous emission lineshape in narrow.

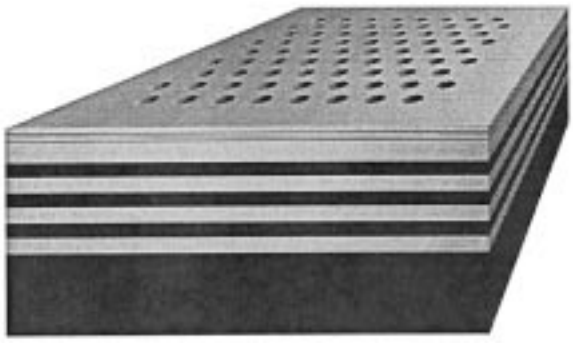

Fig. 12. Low-$Q$ structure: photonic crystal slab without defect, placed on top of a distributed Bragg reflector (DBR).

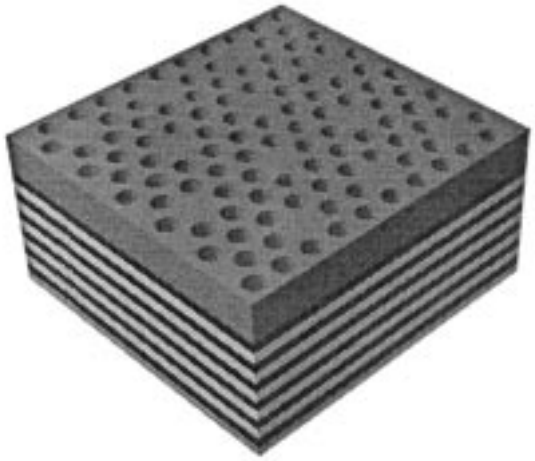

Fig. 13. High-$Q$ structure: photonic crystal slab with defects, placed on top of a DBR substrate.

## IV. Discussion of Different Photonic Crystal LED Structures

Based on the previous discussions, it seems advantageous, depending upon the material characteristics, to use either a low-$Q$ or a high-$Q$ photonic crystal geometry. The low-$Q$ geometry will be advantageous for material systems with a large emission bandwidth or strong photon reabsorption, such as some semiconductor-based emission systems, while the high-$Q$ geometry will be advantageous for material systems with a narrow emission bandwidth or weak photon reabsorption, such as those based on organic emitters.

An example of a low-$Q$ photonic crystal geometry is shown in Fig. 12. A photonic bandgap is created in a guiding layer by introducing a perfectly periodic array of holes. A mirror is introduced to ensure that the output would come out only from the top surface. An active region is incorporated inside the guiding layer. Note that a bandgap in the guided mode spectrum can be opened up, even in the case where the holes do not go through the active region. Therefore, no active material needs to be removed, and the entire active region experiences the effect of the photonic bandgap. In this structure, no cavity is introduced, and the quality factor can, therefore, be made rather low. Such a de-

sign could be suitable for some semiconductor based emitters when photon reabsorption is very significant.

Examples of photonic crystal LED structures incorporating high-$Q$ cavities are shown in Fig. 13. Fig. 13 shows a photonic crystal structure that is similar to the structure depicted in Fig. 12, except that an array of point defects have been introduced in the lattice of holes. A quality factor of several thousand may be achieved using this design. However, since the mode is highly confined around the point defects, only a small portion of the active region is affected by the defect mode and the achievable enhancement is limited. Alternatively, a preferred embodiment might be a configuration where the cavity is created by sandwiching the guiding layer between two DBRs with no point defect introduced in the guiding layer. In this case, the entire active region experiences the effect of the cavity and maximum enhancement is expected.

## V. Conclusion

In conclusion, we analyzed the performance characteristics of photonic crystal LEDs, taking into account the effects of both nonradiative recombination and the photon reabsorption processes. We showed that the design criteria for such an LED are strongly dependent upon the emission lineshapes and material absorption. These results will hopefully be useful as a guidance for achieving high efficiency and modulation rate photonic-crystal LEDs.

## Acknowledgment

The authors acknowledge useful discussions with E. Yablonovitch, H. A. Haus, E. Ippen, and E. F. Schubert.

## References

[1] S. Fan, P. R. Villeneuve, J. D. Joannopoulos, and E. F. Schubert, "High extraction efficiency of spontaneous emission from slabs of photonic crystals," *Phys. Rev. Lett.*, vol. 78, pp. 3294–3297, 1997.

[2] J. D. Joannopoulos, R. D. Meade, and J. N. Winn, *Photonic Crystal*. Princeton, NJ: Princeton Univ. Press, 1995.

[3] R. Coccioli, M. Boroditsky, K. W. Kim, Y. Rahmat-Samii, and E. Yablonovitch, "Smallest possible electromagnetic mode volume in a dielectric cavity," *Proc. IEE—Optoelectronics*, vol. 145, pp. 391–397, 1998.

[4] M. Boroditsky, R. Vrijen, T. F. Krauss, R. Coccioli, R. Bhat, and E. Yablonovitch, "Spontaneous emission extraction, and Purcell enhancement, from thin-film 2-d photonic crystals," *J. Lightwave Technol.*, vol. 17, pp. 2096–2112, Nov. 1999.

[5] H. Yokoyama and S. D. Brorson, "Rate equation analysis of microcavity lasers," *J. Appl. Phys.*, vol. 66, pp. 4801–4805, 1989.

[6] G. Bjork and Y. Yamamoto, "Analysis of semiconductor microcavity lasers using rate equations," *IEEE J. Quantum Electron.*, vol. 27, pp. 2386–2396, Nov. 1991.

[7] H. Yokoyama, H. Yokoyama, and K. Ujihara, Eds., *Spontaneous Emission and Laser Oscillation in Microcavities*. Boca Raton, FL: CRC Press, 1995, ch. 8.

[8] R. Loudon, *The Quantum Theory of Light*. Oxford, U.K.: Oxford Univ. Press, 1983, ch. 1.

[9] H. C. Casey Jr. and M. B. Panish, *Heterostructure Lasers Part A: Fundamental Principles*. New York: Academic, 1978, ch. 3.

[10] G. Bjork and Y. Yamamoto, *Spontaneous Emission and Laser Oscillation in Microcavities*, H. Yokoyama and K. Ujihara, Eds. Boca Raton, FL: CRC Press, 1995, ch. 6.

[11] M. Berggren, A. Dodabalapur, R. E. Slusher, and Z. Bao, "Light amplification in organic thin films using cascade energy transfer," *Nature*, vol. 389, pp. 466–469, 1997.

[12] V. Bulovic, A. Shoustikov, M. A. Blado, E. Bose, V. G. Kozlov, M. E. Thompson, and S. R. Forrest, "Bright, saturated, red to yellow organic light-emitting devices based on polarization induced spectral-shifts," *Chem. Phys. Letts.*, vol. 287, pp. 455–460, 1998.

[13] G. H. B. Thompson, *Physics of Semiconductor Laser Devices*. Chichester, U.K.: Wiley, 1980, p. 56.

[14] J. S. Foresi, P. R. Villeneuve, J. Ferrara, E. R. Thorn, G. Steinmeyer, S. Fan, J. D. Joannopoulos, L. C. Kimerling, H. I. Smith, and E. P. Ippen, "Measurement of photonic band gap waveguide microcavities," *Nature*, vol. 390, pp. 143–145, 1997.

[15] I. Schnitzer, E. Yablonovitch, C. Caneau, and T. J. Gmitter, "Ultrahigh spontaneous emission quantum efficiency, 99.7% internal and 72% external, from AlGaAs/GaAs/AlGaAs double heterostructures," *Appl. Phys. Lett.*, vol. 62, pp. 131–133, 1993.

[16] R. K. Lee, O. J. Painter, B. D'Urso, A. Scherer, and A. Yariv, "Measurement of spontaneous emission from a two-dimensional photonic band gap defined microcavity at near-infrared wavelengths," *Appl. Phys. Lett.*, vol. 74, pp. 1522–1524, 1999.

[17] T. F. Krauss, B. Vogele, C. R. Stanley, and R. M. De La Rue, "Waveguide microcavity based photonic microstructures," *IEEE Photonics Technol. Lett.*, vol. 9, pp. 176–178, Feb. 1997.

[18] F. P. Schäfer, Ed., *Dye Lasers*. Berlin, Germany: Springer-Verlag, 1990.

**Shanhui Fan**, photograph and biography not available at the time of publication.

**Pierre R. Villeneuve**, photograph and biography not available at the time of publication.

**J. D. Joannopoulos**, photograph and biography not available at the time of publication.